34th Annual International Conference of the IEEE EMBS
San Diego, California USA, 28 August - 1 September, 2012

Global Optimization for Human Skin Investigation in Terahertz

Bao C. Q. Truong[1], H. D. Tuan[1], H. H.Kha[1] and H.T. Nguyen[1]

Abstract— **In this paper, the electromagnetic interaction between human skin and terahertz radiation is investigated through the double Debye parameters' extraction algorithm. The changes of skin content are contrasted at the frequencies below one terahertz(THz) but the recent approaches could provide only a rough estimation. We propose an global optimization based identification, which results in globally accurate estimators in the frequency range up to two THz, and thus supports the validity of Debye model for Terahertz wave's propagation and reflection in skin. Simulation results confirm our prominent methodology.**

I. INTRODUCTION

THz imaging and spectroscopy have drew the attention from researchers since the last decade [1], [2]. The attractive properties of THz radiation include non-ionization, low photon energy (below 40 meV) and high water absorption. The high sensitivity of terahertz radiation to polar liquid is the key for THz applications. In particular, the early skin cancer diagnosis can be based on THz radiation pattern because most of biological tissues have a considerably-high proportion of water. In fact, the T-ray imaging systems with its THz pulse imaging (TPI) and continuous-wave (CW) terahertz imaging have been applied in cancer detection [3]–[5]. Both these THz imaging components provide the contrast images of various biological tissue due to changes in their hydration profile [6]. On the other hand, the THz time-domain spectroscopy system is utilized for revealing the interaction between THz radiation and biological tissue, and also the impact of material content on the response of THz waves [7], [8].

In regard to electromagnetic interaction between the skin tissue and THz radiation, terahertz spectroscopy is a dominant tool to develop the knowledge. The data acquisition of the terahertz technique can be represented as optical and dielectric constants. We shall investigate the double Debye model [9], [10], which is a simple dielectric frequency function involving five independent parameters for expression of the dispersions and relaxation times of two Debye relaxation processes in the THz regime. As can be seen in [11], there is a great deal of potential contrast through the extracted double Debye parameters of healthy and cancerous skin. Indeed, the higher dispersion of basal cell carcinoma (BCC) than normal skin (NS) is well reflected in the extracted parameters characterizing dispersive property in the double Debye model. The importance of the double Debye system identification corresponding to modelling the interaction between THz radiation and human skin is supported by [11]–[13]. However, the existing identification procedures employing nonlinear least square are not quite satisfactory in terms of optimality and consistency. The results of [9], [10], [14] could provide an analytical double Debye model, which shows a good agreement with its measured frequency responses at only selective frequencies below one THz. However the estimation of [15], which considered the frequency responses at wider ranged frequencies up to two THz, appeared to be worse than its counterparts [9], [10], [14]. A suggestion about an addition of two Lorentzian resonant process terms to the double Debye model is proposed by [9] to maintain the accurate estimation of their non-linear least square method, whenever frequency range is extended to two THz. These additional terms may result in the more complexity for modeling problem. The question is whether the double Debye model is able to accurately describe the interaction between THz radiation and human skin in the THz frequency range up to two THz and it remains open.

In this paper we give a positive answer to this questions by a new technique for identifying these five parameters of double Debye model. The conventional least square error function, on which the identification is based, is a complex nonlinear and nonconvex function in these five parameters, so the mentioned nonlinear square based approach could locate a solution to satisfy only some necessary optimality conditions. Its inconsistent performance implies that the found solution is not optimal at all. In contrast, our approach locates the global optimal solution of this nonlinear least square error, which leads to the optimal Debye model for a very accurate description of the interaction between terahertz radiation and human skin in the THz frequencies within two THz. Obviously, the least square error is only one of other criteria in parameter identification. The key point of this work is employing the branch and bound algorithm proposed by [16], [17] in order to simultaneously search and narrow the optimal location through iterative steps. This method allow users to obtain the optimal solution with a very small adjustable tolerance.

The paper is structured as follows. Section 2 is devoted to the problem formulation whereas Section 3 provides a development of our global optimization technique for its solution. Preliminary simulations are given in Section 4. Section 5 concludes the paper.

The notations used in the paper are rather standard. Particularly, the notation $A \succeq 0$ means A is a positive semi-definite matrix. For $x = (x_1, x_2)^T \in R^2$ and $p = (p_1, p_2) \in R^2$, $q = (q_1, q_2) \in R^2$, the notations $x \geq p$ and $x \in [p, q]$ are component-wise understood, i.e. they mean $x_i \geq p_i$ and

[1]Centre for Health Technology, Faculty of Engineering and Information Technology, University of Technology, Sydney, AUSTRALIA; Email: cao.q.truong@student.uts.edu.au, {tuan.hoang,khahoang.ha,hung.nguyen}@uts.edu.au

$x_i \in [p_i, q_i]$ for all $i = 1, 2$, respectively. For simplicity we write $x \geq 0$ to refer $x_i \geq 0$, $i = 1, 2$, and accordingly $R^2_+ = \{x \in R^2 \ : \ x_i \geq 0, \ i = 1, 2\}$.

II. MODEL AND PROBLEM IDENTIFICATION

In general, the permittivity is obtained through the following steps (see e.g. [12], [14], [18] and references therein). Firstly, the THz time-domain spectroscopy generates the THz pulse in the reflection or transmission geometry. A transmission or reflection coefficient is then defined by the deconvolution of the measured THz pulse with the sample and without the sample in the frequency domain. These coefficients are inserted into the numerical estimation proposed by [18] in order to extract the frequency-dependent complex refractive index precisely over the examining range of frequency. The reliable approaches to extract these values in frequencies can be also found in [19]–[21]. The extracted values of refraction are the real refractive index $\boldsymbol{n}(\omega)$ and the extinction coefficient $\boldsymbol{\kappa}(\omega)$. Accordingly, the relative complex permittivity $\tilde{\varepsilon}_r$ is defined as

$$\tilde{\varepsilon}_r(\omega) = (\boldsymbol{n}(\omega) - \jmath\boldsymbol{\kappa}(\omega))^2. \tag{1}$$

On the other hand, the double Debye model describing this relative complex permittivity [10] is

$$\tilde{\varepsilon}_r(\omega) = \boldsymbol{\varepsilon}_\infty + \frac{\boldsymbol{\varepsilon}_1}{1 + \jmath\omega\boldsymbol{\tau}_1} + \frac{\boldsymbol{\varepsilon}_2}{1 + \jmath\omega\boldsymbol{\tau}_2}. \tag{2}$$

Here $\boldsymbol{\varepsilon}_\infty \geq \varepsilon_0 := 1$ is the limiting value at high frequency of the permittivity $\tilde{\varepsilon}_r(\omega)$, $\boldsymbol{\varepsilon}_s \geq \varepsilon_0 := 1$, $\boldsymbol{\varepsilon}_1 := \boldsymbol{\varepsilon}_s - \boldsymbol{\varepsilon}_{in} \geq 0$ and $\boldsymbol{\varepsilon}_2 := \boldsymbol{\varepsilon}_{in} - \boldsymbol{\varepsilon}_\infty \geq 0$ represent the dispersion in the amplitude of the slow relaxation process, where the bulk bonding between hydrogen molecules is released to equilibrium statement, and the fast relaxation process, where the molecular reorientation of hydrogen-bonding occurs. $\boldsymbol{\tau}_1$ is the relaxation time of the slow process and $\boldsymbol{\tau}_2$ is the relaxation time of the fast process. $\epsilon_0 = 1$ is the permittivity of vacuum.

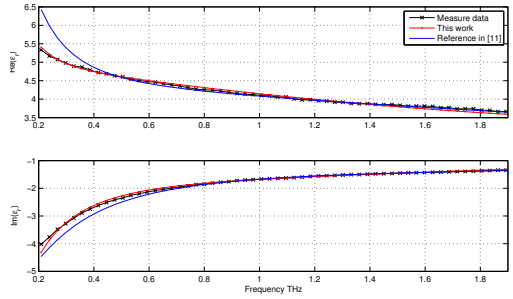

Fig. 1. The real and imaginary part of the relative permittivity of normal skin in [11] plotted by: The extracted data of [11], the double Debye model obtained by BB optimization and by [11].

To identify the double Debye model from the measured data, i.e. to identify its five parameters $\boldsymbol{\varepsilon}_\infty, \boldsymbol{\varepsilon}_1, \boldsymbol{\varepsilon}_1, \tau_1, \tau_2$ based on its measured frequency responses $\tilde{c}_i = \tilde{\varepsilon}_r(\omega_i)$, we use the square error

$$E(\omega_i) = \left| \boldsymbol{\varepsilon}_\infty + \frac{\boldsymbol{\varepsilon}_1}{1 + \jmath\omega_i\boldsymbol{\tau}_1} + \frac{\boldsymbol{\varepsilon}_2}{1 + \jmath\omega_i\boldsymbol{\tau}_2} - \tilde{c}_i \right|^2. \tag{3}$$

Accordingly, $(\boldsymbol{\varepsilon}_1, \boldsymbol{\varepsilon}_2, \boldsymbol{\varepsilon}_\infty, \boldsymbol{\tau}_1, \boldsymbol{\tau}_2)$ is identified from the following total square error minimization

$$\min_{(\boldsymbol{\varepsilon}_1, \boldsymbol{\varepsilon}_2, \boldsymbol{\varepsilon}_\infty, \boldsymbol{\tau}_1, \boldsymbol{\tau}_2)} \sum_{i=1}^{N} E(\omega_i) \tag{4a}$$

$$\text{subject to} \quad \boldsymbol{\varepsilon}_\infty \geq \varepsilon_0, \boldsymbol{\varepsilon}_1 \geq 0, \ \boldsymbol{\varepsilon}_2 \geq 0, \boldsymbol{\tau}_1 > 0, \boldsymbol{\tau}_2 > 0, \tag{4b}$$

where N is the number of discrete samples in the considering range of frequency. The constraints in (4) cover most practical cases of dispersive materials and can be explained from the physical viewpoint [10]. Additionally, for human skin [10], [11], [14], [15],

$$\begin{aligned} l_1 := 1ps \leq \boldsymbol{\tau}_1 \leq u_1 := 20ps, \\ l_2 := 0.01ps \leq \boldsymbol{\tau}_2 \leq u_2 := 0.5ps. \end{aligned} \tag{5}$$

To realize the complexity of program (4)-(5) we now derive the explicit form of its objective function. Set $0 < a_i := \text{Re}(\tilde{c}_i)$, $0 < b_i := -\text{Im}(\tilde{c}_i)$, $\gamma = \sum_{i=1}^{N}(a_i^2 + b_i^2)$, and $x = (\boldsymbol{\varepsilon}_1, \boldsymbol{\varepsilon}_2, \boldsymbol{\varepsilon}_\infty)^T$ as well as $f_i(\tau_1, \tau_2) := (\frac{1}{1+\omega_i^2\tau_1^2}, \frac{1}{1+\omega_i^2\tau_2^2}, 1)^T$, $g_i(\tau_1, \tau_2) := (\frac{\omega_i\tau_1}{1+\omega_i^2\tau_1^2}, \frac{\omega_i\tau_2}{1+\omega_i^2\tau_2^2}, 0)^T$. Then

$$\begin{aligned} E(x, \tau_1, \tau_2) \ = \ & x^T(\Gamma(\tau_1, \tau_2) + \Lambda(\tau_1, \tau_2))x \\ & + (\beta(\tau_1, \tau_2) + \chi(\tau_1, \tau_2))^T x + \gamma \end{aligned} \tag{6}$$

where $\Gamma(\tau_1, \tau_2) := \sum_{i=1}^{N} \Gamma_i(\tau_1, \tau_2)$, $\Lambda(\tau_1, \tau_2) = \sum_{i=1}^{N} \Lambda_i(\tau_1, \tau_2)$, $\beta(\tau_1, \tau_2) = \sum_{i=1}^{N} \beta_i(\tau_1, \tau_2)$, $\chi(\tau_1, \tau_2) = \sum_{i=1}^{N} \chi_i(\tau_1, \tau_2)$, with $\Gamma_i(\tau_1, \tau_2) = f_i(\tau_1, \tau_2) f_i^T(\tau_1, \tau_2)$, $\Lambda_i(\tau_1, \tau_2) = g_i(\tau_1, \tau_2) g_i^T(\tau_1, \tau_2)$, $\beta_i(\tau_1, \tau_2) = -2a_i f_i(\tau_1, \tau_2)$, $\chi_i(\tau_1, \tau_2) = -2b_i g_i(\tau_1, \tau_2)$. Program (4)-(6) is briefly rewritten by

$$\min_{x=(\boldsymbol{\varepsilon}_1, \boldsymbol{\varepsilon}_2, \boldsymbol{\varepsilon}_\infty), \boldsymbol{\tau}_1, \boldsymbol{\tau}_2} E(x, \tau_1, \tau_2) \ : \ (4b), (5), \tag{7}$$

which is recognized as highly nonconvex [17].

III. OPTIMIZATION ALGORITHM

Our key observation is that the objective function in (7) is obviously convex and quadratic in $x = (\boldsymbol{\varepsilon}_1, \boldsymbol{\varepsilon}_2, \boldsymbol{\varepsilon}_\infty)^T$ with τ_1 and τ_2 held fixed. Thus, we can rewrite (4) into the parametric optimization in $\tau = (\tau_1, \tau_2)$

$$\min_{\tau=(\tau_1, \tau_2)} F(\tau_1, \tau_2) \quad \text{subject to} \quad (5) \tag{8}$$

with

$$F(\tau_1, \tau_2) = \min_{x=(\boldsymbol{\varepsilon}_1, \boldsymbol{\varepsilon}_2, \boldsymbol{\varepsilon}_\infty)} E(x) : \ \boldsymbol{\varepsilon}_\infty \geq \varepsilon_0, \ \boldsymbol{\varepsilon}_1 \geq 0, \ \boldsymbol{\varepsilon}_2 \geq 0. \tag{9}$$

Since $\Gamma(\tau_1, \tau_2) \succeq 0$ and $\Lambda(\tau_1, \tau_2) \succeq 0$ for every (τ_1, τ_2) the computation for $F(\tau_1, \tau_2)$ can be performed by an existing quadratic solver such as SeduMi in just three dimensional variable $x \in R^3_+$ [22]. However, the objective function $F(\tau_1, \tau_2)$ is highly nonconvex and nondifferentiable so (8)

is still computationally intractable. We now present a branch and bounding method of global optimization [17] for computational efficiency. Using the monotonic concepts in [23], it is

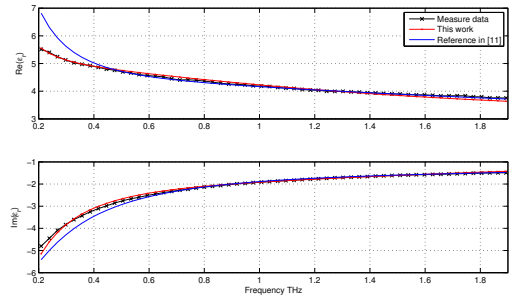

Fig. 2. The real and imaginary part of the relative permittivity of basal cell carcinoma (BCC) in [11] plotted by: The extracted data of [11], the double Debye model obtained by BB optimization and by [11].

easily seen that whenever $(\tau_1, \tau_2) \in [p, q]$ with $p = (p_1, p_2)$ and $q = (q_1, q_2)$,

$$E_1(\omega_i) \geq F_i(\boldsymbol{\epsilon}_1, \boldsymbol{\epsilon}_2, \boldsymbol{\epsilon}_\infty) := x^T \Upsilon_i(q) x + \xi_i^T(p) x + a_i \quad (10)$$

for $\Upsilon_i(q) = f_i(q) f_i^T(q), \xi_i(p) = -2a_i f_i(p)$. Since the

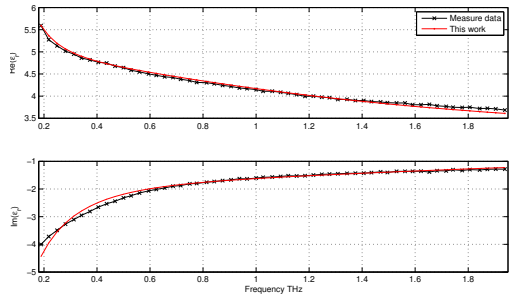

Fig. 3. The real and imaginary part of the relative permittivity of normal skin of the case 266 of [24] plotted by: The extracted data of [24] and the double Debye model obtained by BB optimization.

function $\left(\frac{\tau_1}{1+\omega_i^2\tau_1^2}\right)$ is decreasing in the considered range of τ_1,

$$E_2(\omega_i) \geq G_i(\boldsymbol{\epsilon}_1, \boldsymbol{\epsilon}_2, \boldsymbol{\epsilon}_\infty) := x^T \Psi_i(p, q) x + \zeta_i(p, q)^T x + b_i^2 \quad (11)$$

with $\Psi_i(p, q) = \bar{g}_i(p, q) \bar{g}_i^T(p, q)$, $\zeta_i(p, q) = -2b_i \bar{g}_i(q, p)$ and $g_i(p, q) = (\frac{\omega_i q_1}{1+\omega_i^2 q_1^2}, \frac{\omega_i p_2}{1+\omega_i^2 p_2 q_2}, 0)^T$, $\bar{g}_i(q, p) = (\frac{\omega_i p_1}{1+\omega_i^2 p_1^2}, \frac{\omega_i q_2}{1+\omega_i^2 p_2 q_2}, 0)^T$.
It then follows that a lower bound of $F(\tau_1, \tau_2)$ in $[p, q]$ is

$$\begin{aligned} \bar{F}(p, q) \quad &:= \min_{x=(\boldsymbol{\epsilon}_1, \boldsymbol{\epsilon}_2, \boldsymbol{\epsilon}_\infty)} \sum_{i=1}^{N} (F_i + G_i) \\ &\text{subject to} \quad \boldsymbol{\epsilon}_\infty \geq \varepsilon_0, \boldsymbol{\epsilon}_1 \geq 0, \ \boldsymbol{\epsilon}_2 \geq 0. \end{aligned} \quad (12)$$

which is a convex quadratic program and can be solved by SeduMi. It is worth mentioning that $\bar{F}(p, q) \nearrow F(\omega_i)$ as $p \nearrow q$ which consists the consistence condition for the convergence of the BB algorithm noted in [16].

With such bounding, the implementation of the BB algorithm is as follows

- *Initialization.* Start with the initial rectangles $M_i = [p^i, q^i]$, $i = 1, 2, ..., 10$. Set $\mathcal{S}_1 = \mathcal{N}_1 = \{M_1, M_2, ..., M_L\}$. Set $\kappa = 1$. Set $\mu = \min_{i=1,2,...,M} F((p+q)/2)$.
- *Step 1.* For each $M = [p, q] \in \mathcal{N}_\kappa$ compute $F((p+q)/2)$ by (9). Update current best value (CBV) $\mu \to F((p+q)/2)$ and current best solution τ_{opt} if $F((p+q)/2) < \mu$. Solve (12) to obtain $L(M) = \bar{F}(p, q)$.
- *Step 2.* Delete all M such that $L(M) \geq \mu - \epsilon$ (ϵ is a given tolerance). Let $\mathcal{R}_\kappa$ be the set of remaining rectangles. If $\mathcal{R}_\kappa = \emptyset$, terminate: μ is the optimal value of (8) with tolerance ϵ.
- *Step 3.* Choose $M_\kappa \in \arg\min\{L(M) : M \in \mathcal{R}_\kappa\}$ and divide it into four smaller rectangles $M_{\kappa,1}, M_{\kappa,2}, M_{\kappa,3}, M_{\kappa,4}$ according to the standard bisection rule, $\tau_i = (q_i - p_i)/2$ with $i = 1, 2$. Let $\mathcal{N}_{\kappa+1} = \{M_{\kappa,1}, M_{\kappa,2}\}$, $\mathcal{S}_{\kappa+1} = (\mathcal{R}_\kappa \setminus M_\kappa) \cup \mathcal{N}_{\kappa+1}$. Set $\kappa \to \kappa + 1$ and go back to Step 1.

IV. NUMERICAL RESULTS AND DISCUSSION

TABLE I
DOUBLE DEBYE PARAMETERS EXTRACTED FROM THE DATA OF [11], [24] IN THIS WORK AND THE CORRESPONDING REFERENCE PARAMETERS

Case	Method	$\boldsymbol{\varepsilon}_s$	$\boldsymbol{\varepsilon}_{in}$	$\boldsymbol{\varepsilon}_\infty$	$\boldsymbol{\tau}_1(ps)$	$\boldsymbol{\tau}_2(ps)$
NS [11]	By [11]	14.7	4.16	2.58	1.45	0.0611
NS [11]	This work	26.03	4.63	2.89	3.84	0.104
BCC [11]	By [11]	17.6	4.23	2.65	1.55	0.0614
BCC [11]	This work	36.71	4.83	2.99	4.86	0.116
NS [24]	This work	24.85	4.7	3.03	3.84	0.1136
BCC [24]	This work	34.3	4.96	2.98	4.08	0.1145

Although each term $F_i(\boldsymbol{\epsilon}_1, \boldsymbol{\epsilon}_2, \boldsymbol{\epsilon}_\infty) + G_i(\boldsymbol{\epsilon}_1, \boldsymbol{\epsilon}_2, \boldsymbol{\epsilon}_\infty)$ is a tight lower bound for $E(\omega_i)$ (see (10) and (9)), their sum through the whole examining range of frequency is obviously much looser lower bound for the objective function $F(\tau_1, \tau_2)$ of (4) on $[p, q]$. This fact should not be a surprise since $F(\tau_1, \tau_2)$ implicitly is a fraction of extremely high order polynomials. Therefore the first step for the implementation of BB algorithm is to iteratively narrow down the area for its branching and bounding by the updated tolerance κ and the terminating condition of BB algorithm. In detail, the tolerance is calculated by the expression $\epsilon = \mu - L(M_\kappa)$ at the step κ where $L(M_\kappa) = \min\{L(M) : M \in \mathcal{R}_\kappa\}$, and thus it terminates the program to obtain a smaller optimal area.

In this paper, we use the data source extracted from [11], [15] [24]. Data acquisition steps for our simulation were introduced in [11], [24] as well. The investigated frequency is chosen from 0.2 to 2 THz due to the useful spectral range documented by [25]. The number N of the taken sampled frequencies is about 57. The particular values of the double Debye parameters extracted by our simulation in various cases are listed in Table. I together with reference values

estimated by [11], [24]. Fig. 1-2 depict the outcomes of of this work in comparison with the reference study, our approach and the so-called measured complex permittivity of various cases of normal skin and BCC. It is obvious that this paper's approach, the BB optimization can procure better agreement with the measured complex permittivity than previous studies especially at the low part of examining range of frequency. The consistent outcomes of the proposed parameter extraction method in this paper can also be seen in Fig. 3-4. Analysing these data in detail, there is a large difference between this work and the reference studies. [11] applied the double Debye parameters extraction method introduced by [10]. However [10] only supposed their estimation for the double Debye model reliable in the frequency range below 1 THz. Therefore extending the estimating frequency up to 2 THz and using the approach of [10] may result in the large deviation between the measured permittivity and the simulated double Debye model.

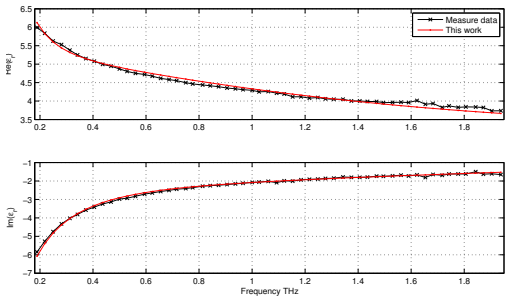

Fig. 4. The real and imaginary part of the relative permittivity of basal cell carcinoma sample of the case 266 of [24] plotted by: The extracted data of [24] and the double Debye model obtained by BB optimization.

V. CONCLUSION

Our estimation results confirm the feasibility of the double Debye's application to describe the complex permittivity of human skin in terahertz regime. BB algorithm, then, can be recognised as an advance technique for parameters extraction when our simulation outcomes illustrate the better estimation than previous studies. From another point of view, our proposed approach enables the classification of different statements of skin thanks to the accurate transformation of data series into finite-dimensional vectors. Furthermore improving the resolution of terahertz spectroscopy system and the complex refractive index extraction procedure is the foundation for further studies about the parameters classification in terms of early skin cancer diagnosis.

REFERENCES

[1] B. B. Hu and M. C. Nuss, "Imaging with terahertz waves," *Opt. Lett.*, vol. 20, pp. 1716–1718, Aug 1995.

[2] E. P. J. Parrott, S. M. Y. Sy, T. Blu, V. P. Wallace, and E. Pickwell-MacPherson, "Terahertz pulsed imaging in vivo: measurements and processing methods," *Journal of Biomedical Optics*, vol. 16, no. 10, p. 106010, 2011.

[3] S. Nakajima, H. Hoshina, M. Yamashita, C. Otani, and N. Miyoshi, "Terahertz imaging diagnostics of cancer tissues with a chemometrics technique," *Applied Physics Letters*, vol. 90, pp. 041102 –041102–3, jan 2007.

[4] R. M. Woodward, B. E. Cole, V. P. Wallace, R. J. Pye, D. D. Arnone, E. H. Linfield, and M. Pepper, "Terahertz pulse imaging in reflection geometry of human skin cancer and skin tissue," *Physics in Medicine and Biology*, vol. 47, no. 21, p. 3853, 2002.

[5] V. P. Wallace, P. F. Taday, A. J. Fitzgerald, R. M. Woodward, J. Cluff, R. J. Pye, and D. D. Arnone, "Terahertz pulsed imaging and spectroscopy for biomedical and pharmaceutical applications," *Faraday Discuss.*, vol. 126, pp. –, 2004.

[6] R. M. Woodward, V. P. Wallace, R. J. Pye, B. E. Cole, D. D. Arnone, E. H. Linfield, and M. Pepper, "Terahertz pulse imaging of ex vivo basal cell carcinoma.," *The Journal of investigative dermatology*, vol. 120, no. 1, pp. 72–78, 2003.

[7] V. P. Wallace, P. F. Taday, A. J. Fitzgerald, R. M. Woodward, J. Cluff, R. J. Pye, and D. D. Arnone, "Terahertz pulsed imaging and spectroscopy for biomedical and pharmaceutical applications," *Faraday Discuss.*, vol. 126, pp. –, 2004.

[8] P. Siegel, "Terahertz technology in biology and medicine," *Microwave Theory and Techniques, IEEE Transactions on*, vol. 52, pp. 2438 – 2447, oct. 2004.

[9] H. J. Liebe, G. A. Hufford, and T. Manabe, "A model for the complex permittivity of water at frequencies below 1 THz," *Inter. J. of Infrared and Millimeter Waves*, vol. 12, pp. 659–675, 1991.

[10] J. Barthel and R. Buchner, "High frequency permittivity and its use in the investigation of solution properties," *Pure and Applied Chemistry*, vol. 63, no. 10, pp. 1473–1482, 1991.

[11] E. Pickwell, A. J. Fitzgerald, B. E. Cole, P. F. Taday, R. J. Pye, T. Ha, M. Pepper, and V. P. Wallace, "Simulating the response of terahertz radiation to basal cell carcinoma using ex vivo spectroscopy measurements," *Journal of Biomedical Optics*, vol. 10, no. 6, p. 064021, 2005.

[12] E. Pickwell, B. E. Cole, A. J. Fitzgerald, M. Pepper, and V. P. Wallace, "In vivo study of human skin using pulsed terahertz radiation," *Physics in Medicine and Biology*, vol. 49, no. 9, p. 1595, 2004.

[13] Z. Taylor, R. Singh, D. Bennett, P. Tewari, C. Kealey, N. Bajwa, M. Culjat, A. Stojadinovic, H. Lee, J.-P. Hubschman, E. Brown, and W. Grundfest, "THz medical imaging: in vivo hydration sensing," *Terahertz Science and Technology, IEEE Transactions on*, vol. 1, pp. 201 –219, sept. 2011.

[14] J. T. Kindt and C. A. Schmuttenmaer, "Far-infrared dielectric properties of polar liquids probed by femtosecond terahertz pulse spectroscopy," *J. Phys. Chem.*, vol. 100, pp. 10373–10379, 1996.

[15] E. Pickwell, B. E. Cole, A. J. Fitzgerald, V. P. Wallace, and M. Pepper, "Simulation of terahertz pulse propagation in biological systems," *Applied Physics Letters*, vol. 84, no. 12, pp. 2190–2192, 2004.

[16] H. D. Tuan, P. Apkarian, S. Hosoe, and H. Tuy, "D.c. optimization approach to robust control: Feasibility problems," *International Journal of Control*, vol. 73, no. 2, pp. 89–104, 2000.

[17] H. Tuy, *Convex Analysis and Global Optimization*. Kluwer Academic, 1998.

[18] T. D. Dorney, R. G. Baraniuk, and D. M. Mittleman, "Material parameter estimation with terahertz time-domain spectroscopy," *J. Opt. Soc. Am. A*, vol. 18, pp. 1562–1571, Jul 2001.

[19] L. Duvillaret, F. Garet, and J.-L. Coutaz, "A reliable method for extraction of material parameters in terahertz time-domain spectroscopy," *IEEE Journal of Selected Topics in Quantum Electronics*, vol. 2, pp. 739 –746, sep 1996.

[20] L. Duvillaret, F. Garet, and J.-L. Coutaz, "Highly precise determination of optical constants and sample thickness in terahertz time-domain spectroscopy," *Appl. Opt.*, vol. 38, pp. 409–415, Jan 1999.

[21] I. Pupeza, R. Wilk, and M. Koch, "Highly accurate optical material parameter determination with thz time-domain spectroscopy," *Opt. Express*, vol. 15, pp. 4335–4350, Apr 2007.

[22] J. F. Sturm, "Using sedumi 1.02, a matlab toolbox for optimization over symmetric cones," *Optimization Methods and Software*, vol. 11, no. 1, pp. 625–653, 1999.

[23] H. Tuy, "Monotonic optimization: Problems and solution approaches," *SIAM Journal on Optimization*, vol. 11, no. 2, p. 464494, 2000.

[24] V. P. Wallace, A. J. Fitzgerald, E. Pickwell, R. J. Pye, P. F. Taday, N. Flanagan, and T. Ha, "Terahertz pulsed spectroscopy of human basal cell carcinoma.," *Applied Spectroscopy*, vol. 60, no. 10, pp. 1127–1133, 2006.

[25] C. D. Sudworth, A. J. Fitzgerald, E. Berry, N. N. Zinov'ev, S. Homer-Vanniasinkam, R. E. Miles, M. Chamberlain, and M. A. Smith, "The optical properties of human tissue at terahertz frequencies," in *Novel Optical Instrumentation for Biomedical Applications*, pp. 5143–51559, Optical Society of America, 2003.